FAULTING PERFORMANCE MODEL FOR UNDOWELED JOINTED CONCRETE PAVEMENTS USING SHRP-LTPP DATABASE

Neeraj Buch, Assistant Professor
Dept. of Civil and Environmental Engineering, Michigan State University

Kim Hyung Bae, Research Assistant
Dept. of Civil and Environmental Engineering, Michigan State University.

ABSTRACT

Joint faulting of undoweled transverse joints contributes to longitudinal roughness, and subsequent user discomfort (poor ride quality) and needs for rehabilitation and repair. In this paper the authors propose two (based on support conditions) joint faulting prediction models based on the Strategic Highway Research Program (SHRP) - Long Term Pavement Performance (LTPP) database. The models consist of explanatory variables like shear capacity, pavement support, temperature, unconfined compressive strength, size ratios, and pavement response. Variables (from the database) like shear capacity, load transfer efficiency, pavement support, and crack widths were back calculated using mechanistic-empirical algorithms for more realistic estimates. Efforts were made to determine the form of the model and explanatory variables that made engineering sense, rather than blindly relying on statistical tools. The paper discusses the methodology used in selecting explanatory variables (independent variables) in the model development and results of the sensitivity analysis. The analysis of the data has shown that undoweled joint faulting is a function of traffic, joint shear capacity, joint spacing, base type and pavement support. The paper provides a comprehensive reliability analysis (with illustrative example) of the models developed.

BACKGROUND

The Long Term Pavement Performance (LTPP) program was started in 1987 as part of the Strategic Highway Research Program (SHRP). The scope of the program was to "*provide the tools for increasing pavement performance and service life in order to better serve the needs of the motoring public, and to provide for the delivery of goods and services without major increases in financial resources*"(1). The database includes a complete inventory on design, construction, and performance characteristics of numerous pavement sections throughout the country. It is a subset of this large database (undoweled jointed concrete pavements) that is being analyzed to develop joint faulting prediction models.

At the conclusion of the P-20 analysis contracts, the data tables were not complete enough and or/ sufficient time had not elapsed for the development of enough distress to calibrate existing fault prediction models. The statistical models developed under SHRP study P-393 had relatively low R^2 values due to these same limitations (2). This report summarized the effects of loading, environment, material properties, construction quality and maintenance levels on pavement distress and performance. Early sensitivity analyses of the LTPP data on the above parameters was reported. The P-393 reports do provide guidelines for the development of future distress prediction models, including sensitivity analysis procedures, and examples of how to perform these analyses on the LTPP data. With the passage of time no efforts have been made (until recently) at the national or state levels to calibrate the existing PCC pavement distress models.

With the database now in its seventh year and the availability of repeated distress (joint faulting) measurements, deflection measurements, traffic data, and environmental data for most of the GPS-3 (JPCP) and GPS-4 (JRCP) test sections enables the pavement designer to better understand the behavior of the prediction models.

Efforts have been made to back calculate variables (from the database) like shear capacity across the joint (function of LTE and joint stiffness), load transfer efficiency (function of deflection), pavement support properties (as a function of deflection, basin area) and crack widths (function of slab length, temperature, and concrete properties) using mechanistic-

empirical algorithms for more realistic estimates, subsequently, these variables have been included in the prediction model. The above mentioned variables are available at repeated intervals in the LTPP database. The paper also provides a framework for reliability analysis (illustrative example included) to be included in an overall pavement design scheme. The intent of this paper is to develop a joint faulting prediction model using sound engineering and statistical modeling concepts, identifying explanatory variables based on the distress mechanism(s).

JOINT FAULTING MECHANISM(S) AND EXISTING SHRP MODEL

Faulting is defined as "vertical displacement (measured in inches or mm) across a PCC slab joint with respect to the position of the slab on the opposing side of the joint" (3). The preliminary analysis of the data has shown that undoweled joint faulting is a function of traffic, precipitation, crack width, temperature variation and subsequent joint movement and base type (unconfined compressive strength). The analysis will also focus on the impact of joint stiffness, shear capacity and load transfer on joint behavior. The model development will also focus on the effects of tire pressure and radius of relative stiffness on the development of load transfer efficiency across the joint.

The existing SHRP undoweled joint faulting model as discussed in the report P-393 is based on the pavement categories GPS-3 (plain jointed) and GPS-4 (reinforced jointed). The SHRP fault prediction model is as follows (2):

$$FAULTND = CESAL^{0.25}\left[\begin{array}{l} -0.0757 + 0.0251 \bullet (AGE)^{0.5} + 0.0013 \bullet \left(\frac{PRECIP}{10}\right)^2 + \\ 0.0012 \bullet \left(\frac{FI \bullet PRECIP}{1000}\right) - 0.0378 \bullet DRAIN \end{array}\right] \quad (1)$$

where:

FAULTND	=	mean transverse non-doweled joint faulting, in.
CESAL =		cumulative 18,000 lbs ESALs in traffic lane, millions.
PRECIP =		mean annual precipitation, in.
AGE	=	age since construction, years.
DRAIN =		1=longitudinal subgrade, 0=otherwise.

Statistics:

N	=	25 sections
R^2	=	0.550
RMSE	=	0.047 inch

The joint faulting model described in Equation 1 does not relate joint shear capacity or load transfer efficiency deflection to faulting. It has been well documented (4, 5) that both LTE and shear capacity are strongly related to joint deterioration and subsequent joint faulting. Other factors like base type, temperature differentials, subgrade support, and unconfined compressive strength of base have a strong influence on joint faulting magnitudes.

DATA SYNTHESIS AND MODEL DEVELOPMENT

The LTPP database included varying amounts and types of data on 69 GPS-4 test sections (JRCP) and 123 GPS-3 test sections (JPCP) (1). The focus of the data synthesis was to identify (based on previous literature and engineering judgement) key variables that were thought to influence joint faulting. The predictor variables are currently available in a wide range of formats. For example concrete strength for every test section is reported in varying formats, such as compressive strength, flexural strength, indirect tensile strength, and elastic modulus. Unfortunately none of these strength parameters are available for all the sections in the experiment. This varying nature of the reporting format calls for the use of existing empirical formulation correlating these strength parameters to one measure of strength. The data from GPS test sections were reviewed in this light to determine if data expected to be significant were missing. As a result of this review test sections with missing traffic data, joint spacing data, faulting data, temperature data and any data relating to base type were not included in the analysis (Tables 1a and 1b summarize the database).

The plot between base type and joint faulting clearly reveals a pattern, pavements resting on crushed aggregate bases illustrated different (higher) magnitudes of faulting than pavements resting on stabilized bases (Figures 1,2,3) with similar levels of traffic. Based on this observation it was decided to develop two models to explain joint faulting of undoweled jointed concrete pavements.

The modulus of subgrade reaction (k) was back calculated as a function of the basin deflection area, elastic modulus of concrete and the radius of relative stiffness. The basin deflection area is a function of the deflection profile obtained from falling weight deflectometer testing. This data was available from the LTPP database. The modulus of subgrade reaction was calculated as follows (6):

$$AREA_{SHRP} = 4+6(d_8/d_o)+5(d_{12}/d_o)+6(d_{18}/d_o)+9(d_{24}/d_o)+18(d_{36}/d_o)+12(d_{60}/d_0) \quad (2)$$

$$l = [\ln\{(60- AREA_{SHRP})/289.708\}/-0.698]^{2.566} \quad (3)$$

$$k = (E_c h^3)/(12(1-\nu^2)l^4) \quad (4)$$

where

d_o-d_{60}	=	deflection sensor positioning,
$AREA_{SHRP}$	=	basin area,
E_c	=	elastic modulus of concrete (LTPP database),
h	=	pavement thickness (LTPP database),
l	=	radius of relative stiffness, and
k	=	modulus of subgrade reaction

The typical range of $AREA_{SHRP}$ for the test sections in this study was 36 to 50, and the typical l values ranged from 18 to 50.

The deflection data from the LTPP database was utilized to compute load transfer efficiency across the joints using Equation 5 (4). The definitions for unloaded and loaded deflections are illustrated in Figure 4.

$$LTE_\delta\ (\%) = \frac{\delta_{unloaded}}{\delta_{loaded}} \bullet 100 \quad (5)$$

where:

$LTE_\delta(\%)$	=	load transfer efficiency.
$\delta_{unloaded}$	=	unloaded deflection measurement, mils.
δ_{loaded}	=	loaded deflection measurement, mils.

Based on the LTE(%)-joint stiffness (AGG) was computed using the relationship illustrated in Figure 5. This relationship is a function of the pavement cross-section and the modulus of subgrade reaction. AGG is a parameter that describes the stiffness of a joint in the FEM program ILLISLAB and is done by assigning a spring constant value. The next step in characterizing the joint movement and behavior was to compute the shear stress (describes the loss of shear stress) across the joint using the following relationship (4):

$$\tau = \frac{\left(\delta_{loaded} - \delta_{unloaded}\right) \bullet AGG}{h} \quad (6)$$

where:

τ	=	shear stress.
h	=	pavement thickness.
AGG	=	joint stiffness.
$\delta_{unloaded}$	=	unloaded deflection measurement.
δ_{loaded}	=	loaded deflection measurement.

The next step in the analysis process was to back-calculate joint width (ω). The joint width, which is a function of slab length, concrete shrinkage properties, thermal expansion, and average temperature variation was calculated using the following relationship (5):

$$\omega = CL(0.5\alpha\Delta T + \varepsilon_s) \quad (7)$$

where

α	=	thermal coefficient of contraction, ε/°F
ε_s	=	drying shrinkage coefficient of concrete,
L	=	transverse joint spacing,
ΔT	=	temperature range, and
C	=	dimensionless adjustment factor.

The cumulative traffic data (KESALs) was based on historical counts since 1988. The prediction model is based on traffic data through 1994. Information regarding temperature variation, base type and thickness and joint spacing was available from the database. Based on the derived and measured data the next step in the analysis was to identify correlated variables and how they would explain the phenomenon of joint faulting.

Model Development

The first step was perform a bivariate correlation analysis between joint faulting and the variables identified earlier in the paper. The correlation coefficient value lies between -1 and +1 denoting strong negative or strong positive relationship. Table 2 summarizes the correlation matrix for the data set on hand. If the p-value was less than 0.05, then the correlation was considered significant. The second step in model building process was to perform diagnostic analysis on the data set to identify "outliers" or significantly influential observations which might influence the variable selection process and the final form of the prediction model. The initial analysis did not reveal any outliers or influential observations.

The purpose of the variable selection process is to obtain a model that best describes the data set with the fewest number of independent variables. One option was to choose the R^2 algorithm for all possible subsets of the database, and then select a model based on the highest R^2. The problem with this process of variable selection is that the R^2 will increase as the number of variables in the subset increase, but the predictive error (MSE) of the model may be minimal for a subset of variables less than those considered for R^2. Hence, a model will have a superficially high R^2 along with a high mean squared error. So with this drawback in mind the best subset of independent variables for the performance models were selected based on the C_p criterion. C_p is a function of the model mean squared error which adjusts for the number of model parameters relative to the number of observations (7). Based on this criteria and the correlation matrix two performance models were selected.

The general functional form of the joint faulting prediction model was as follows:

$$FAULTD_{SHRP} = KESAL_p \times [\text{Explanatory Variables}] \quad (8)$$

Based on previous studies it has been shown that joint faulting increases rapidly with traffic loading initially, and then levels off at a much decreased rate (2). The model in Equation 8 meets the logical boundaries with faulting equal to zero for zero traffic loading (prior to opening). The coefficients of the prediction model were determined by using the non-regression algorithm in the statistical package SPSS® (7). The final form of the two transverse joint faulting models are as follows:

$$FAULTND_{crushedstone} = \left(\frac{KESAL}{k \bullet PCC}\right)^{0.274} \times \left(76.622 - \tau^{0.749} + \frac{1}{T^{0.329}}\right) \quad (9)$$

Statistics

R^2	=	0.70
F-value	=	4.922
p-value	=	0.02

$$FAULTND_{stabilized} = \left(\frac{KESAL}{k \bullet PCC}\right)^{1.795} \times \left(-1.824 + \tau^{0.104} + \frac{1}{q_u^{0.124}}\right) + 11.827 \quad (10)$$

Statistics

R^2	=	0.80
F-value	=	7.922
p-value	=	0.002

where:

FAULTND	=	mean transverse non-doweled joint faulting.
KESAL	=	cumulative 18,000 lbs ESALs in traffic lane.
k	=	modulus of subgrade reaction.
T	=	$Temp_{max}$-$Temp_{min}$.
τ	=	shear stress (Equation 6).
PCC	=	pavement thickness.
q_u	=	unconfined compressive strength.

Tables 3a and 3b compare the measured faulting levels to the predicted faulting magnitude based on the two regression equations The sensitivity of the two performance models expressed in Equations 9 and 10 are illustrated in Figures 6 through 13. From these plots it is evident that faulting is dependent on traffic levels and pavement thickness irrespective of the subbase support type. It is also evident from the plots that if the joint has adequate load transfer/shear capacity, then the magnitude of faulting is diminished. Pavements resting on stabilized bases are not very sensitive to the modulus of subgrade reaction (k), whereas, pavements founded on aggregate bases are sensitive to the modulus of subgrade reaction.

APPLICATION OF RELIABILITY TO FAULTING MODELS

Since there is uncertainty in the major parameter values of pavements, it is reasonable to define each parameter as a random variable with the complete probability distribution. Once the probability density function (pdf) for each random variable X_i is defined, one can, in concept, produce the pdf for a performance function which is the estimated faulting on this study. The distance between the amount of the maximum allowable faulting (F_{max}) and that of the estimated faulting (F) may be defined as the safety margin (SM) (8) :

$$SM = F_{max} - F \quad (11)$$

If the condition of the limit state, which is defined as a state of the structure including parameters at which the structure is just on the point of not satisfying the requirement, is taken as SM = 0, the area of pdf below the limit state is the probability of failure, Pr(f).

Theoretically, the probability of unsatisfactory performance can be determined by constructing a pdf on the performance function (e.g. SM or ln SM) and calculating the value that is less than that of the limit state. However, Pr(U) is not practical in pavement design because of the incomplete probability information of the design parameters. Even though the probability information of all parameters can be perfectly obtained, the shape of the probability distribution of the performance function which is likely to be non-linear may be difficult to obtain. Practically, approximate moments of the performance function (E[SM] and σ_{SM}) can be obtained from the estimated moments of the parameters of pavements. Using the approximate moments of the performance function, the reliability index, β can be calculated. In other words, reliability can be characterized by the reliability index, β which is the number of standard deviations by which the expected value of the performance function exceeds the limit state. Figure 14 illustrate the concepts of the probability of unsatisfactory performance and the reliability index. Engineering system and components with higher β values are considered more reliable than those with lower value. The reliability index β is a convenient and valid comparative measure of an engineering system that reflects both the mechanics of the problem and uncertainty in the input variables.

Illustrative Example

Based on Equations 9 and 10 the approximate mean value of faulting is:

$$m_{FAULTND_{crushedstone}} = \left(\frac{m_{KESAL}}{m_k \bullet m_{PCC}}\right)^{0.274} \times \left(76.22 - m_\tau + \frac{1}{m_{T^{0.329}}}\right) \quad (12)$$

$$m_{FAULTND_{stabilized}} = \left(\frac{m_{KESAL}}{m_k \bullet m_{PCC}}\right)^{1.795} \times \left(-1.824 + m_\tau + \frac{1}{m_{q^{0.124}{}_u}}\right) + 11.827 \quad (13)$$

Based on the mean values of the random variables, the approximate mean values of faulting are 1.91 mm (75.431 mils) (crushed-stone) and 0.35 mm (13.935 mils) (stabilized).

The next step in reliability process is to determine the partial derivative of the performance function for each random variable. Using those partial derivatives calculated at the mean values of random variables and covariance matrix, the standard deviation of faulting is 18.895 (crushed-stone) and 4.086 (stabilized).

Based on the mean value and standard deviation of the performance functions of faulting, the reliability index can be calculated. First, the expected value of the safety margin is determined by :

$$E[SM] = m_{\max} - m_{faulting} \quad (14)$$

where :

$m_{\max}$ = maximum allowable faulting.

In this study, considering the range of actual field data by which the performance function is modeled and avoiding the erroneous result corresponding to the extrapolation of the estimated values, the maximum allowable faulting is taken as 1.27 mm (50 mils). Since the maximum allowable faulting has zero standard deviation, the standard deviation of the safety margin can be considered as that of the performance function of faulting (8):

$$\sigma_{SM} = \sigma_{faulting} \quad (15)$$

Finally, the reliability index of the performance function of faulting in undoweled PCC pavements can be expressed as (8):

$$\beta_{faulting} = \frac{m_{\max} - m_{faulting}}{\sigma_{faulting}} \quad (16)$$

For crushed stone base $m_{\max}$ = 4.47 mm (176 mils), $m_{faulting}$ = 1.91 mm (75.43 mils) and $\sigma_{faulting}$ = 0.48 mm (18.89 mils), $\beta_{faulting}$ = 5.34, whereas, for stabilized base $m_{\max}$ = 1.27 mm (50 mils), $m_{faulting}$ = 0.35 mm (13.93 mils) and $\sigma_{faulting}$ = 0. 1mm (4.08 mils), $\beta_{faulting}$ = 8.84.

For assumed normality, the simple relationship for the probability of unsatisfactory performance, Pr(U) can be obtained in terms of reliability index (8):

$$\Pr(U) = F_U\left(\frac{0 - E[SM]}{\sigma_{SM}}\right) = F_U(-\beta) \quad (17)$$

where F_U = the cumulative distribution function of a unit normal variate. For the reliability index of 5.34 the Pr(U) is determined as 0.001 and for the reliability index of 8.84 the Pr(U) is determined as 0.0005 .

CONCLUSIONS

Since the SHRP P-393 study this research project was the first attempt towards developing empirical-mechanistic distress prediction models. With the database in its 7th version provided more of the missing information which plagued the earlier versions and the data attempted to better explain joint faulting mechanism(s). With the passage of time and additional information more accurate coefficient predictions can be made with a low level of unexplainable error in the model.

The proposed prediction models have an improved R^2 when compared to the model published in the SHRP P-393 study. The models consist of explanatory variables like shear capacity and pavement support which were back-calculated on sound principles mechanics, size ratios, and pavement response. Efforts were made to determine the form of the model and explanatory variables that made engineering sense, rather than blindly relying on statistical tools. The paper provides a comprehensive reliability design framework for the performance models developed. Based on the reliability analysis both performance equations have a high reliability index and low probability of erroneous prediction.

As more data is collected over time, pavement engineers will be in a position to improve upon the existing models and the associated reliability index by calibrating the coefficients. Other variables like shoulder type, freezing index, etc. can be investigated and incorporated into the model and further explain joint faulting manifestation. At the time of developing this proposed model enough information was not available to justify their inclusion.

Table 1a. Undoweled Pavements on Crushed Stone Bases

STATE	LTE	KESALs	Fault, mm	k, kPa/cm	PCC, mm	Base, mm	Base Type	Joint Spacing, m	Prec, mm	T,°F
Alabama	84.4	5101	5.24	428.97	254.00	152.40	CS	6.10	5491.25	25.4
California	82.56	10452	1.42	838.94	289.56	137.16	CS	4.72	1087.65	19.8
North Dakota	83.13	433	0.62	366.53	203.20	101.60	CS	4.57	1570.50	16.7
Puerto Rico	75.92	17280	3	654.32	251.46	203.20	CS	6.00	6834.72	21.6
Puerto Rico	76.18	4754	4	543.00	228.60	152.40	CS	6.00	5954.80	21.5
Texas	90.19	8532	1	458.84	241.30	127.00	CS	4.57	2591.07	31.5
Washington	83.89	5870	0.35	556.58	198.12	76.20	CS	3.81	3585.36	24.4
Washington	88.89	2424	2.79	521.28	254.00	127.00	CS	3.47	1659.40	18.9
Washington	86.72	1271	0.23	233.49	254.00	127.00	CS	4.72	660.67	25.5
Washington	82.16	2120	0.67	236.78	228.60	50.80	CS	3.51	672.60	14.5
Washington	88.61	8986	0.12	366.53	198.12	60.96	CS	3.51	3744.04	20
Washington	81.91	3014	3.82	285.08	228.60	152.40	CS	4.57	4129.42	23.1
Washington	80.97	4391	0.09	434.40	279.40	152.40	CS	4.72	632.33	30.5
Wisconsin	84.66	11480	6.97	570.15	203.20	203.20	CS	3.51	2000.00	22.9
Wisconsin	83.58	3896	4.48	377.39	254.00	228.60	CS	4.72	3691.00	24.3
Wisconsin	82.66	4591	1.15	437.12	177.80	152.40	CS	4.66	3295.69	26
Wisconsin	82.52	7215	2.16	526.71	228.60	152.40	CS	4.54	3350.86	27

Table 1b. Undoweled Pavements on Stabilized Bases

STATE	LTE	KESALs	Fault, mm	k, kPa/cm	PCC, mm	Base, mm	Base Type	Joint Spacing, m	Prec, mm	T, °F
California	84.59	2137.00	0.29	532.14	198.12	121.92	CA	4.72	1995.00	20.20
California	82.40	8439.00	0.25	477.84	243.84	137.16	CA	4.11	1062.73	23.70
California	77.71	20584.00	0.21	904.095	198.12	106.68	CA	4.72	2544.37	25.50
California	81.07	19804.00	0.09	103.17	228.6	137.16	CA	4.72	1807.75	24.50
California	88.31	7451.00	0.11	268.785	243.84	114.3	CA	4.72	1555.75	27.30
Georgia	86.73	10922.00	1.42	176.475	254	152.4	CA	5.94	4751.06	26.30
Georgia	81.26	16082.00	0.8	447.975	254	152.4	CA	5.94	4894.94	28.70
Nebraska	86.01	4114.00	0.06	453.405	304.8	101.6	CA	4.72	2669.86	26.90
Nevada	88.15	3624.00	3.09	312.225	228.6	152.4	CA	4.72	1126.56	21.60
Nevada	79.90	5104.00	0.78	1001.835	203.2	101.6	CA	4.72	595.20	21.20
California	84.24	8278.00	0.27	188.3124	243.84	121.92	LC	4.11	999.20	20.80
Colorado	80.96	3060.00	0.41	942.105	203.2	101.6	LC	4.72	1414.00	20.70
North Carolina	80.61	2967.00	1.71	371.955	228.6	101.6	LC	4.27	4442.00	20.40
Utah	78.61	2800.00	0.82	412.68	279.4	190.5	LC	4.57	1391.80	23.80
Utah	80.76	2000.00	0.03	662.46	254	101.6	LC	3.81	1247.00	26.00
Utah	78.36	2000.00	0.15	1009.98	228.6	121.92	LC	3.81	630.50	24.70
Wisconsin	84.54	977.00	0.26	754.77	228.6	101.6	LC	4.66	2947.00	22.70

Table 2a. Correlation Coefficients for Aggregate Base Model

Variable	Correlation Coefficient
KESALs	0.794
PCC	0.889
k	0.632
T	0.837
τ	0.78

Table 2b. Correlation Coefficients for Stabilized Base Model

Variable	Correlation Coefficient
KESALs	0.694
PCC	0.841
k	0.642
q_u	0.773
τ	0.855

Table 3a. Inputs for Pavements on Crushed Bases

KESAL	k, kPa/cm	PCC, mm	T, °F	Shear stress, kPa	Fault, mm	Predicted, mm	Residual
5101	428.97	254	28.3	1241.38	5.24	5.03	0.21
10452	838.94	289.56	25.4	346.34	1.42	1.99	-0.57
433	366.53	203.2	19.8	565.93	0.62	0.99	-0.37
17280	654.32	251.46	16.7	142.34	3	2.94	0.06
4754	543.00	228.6	21.6	174.34	4	4.24	-0.24
8532	458.84	241.3	21.5	804.83	1	1.14	-0.14
5870	556.58	198.12	31.5	944.83	0.35	1.07	-0.72
2424	521.28	254	24.4	613.79	2.79	2.26	0.53
1271	233.49	254	18.9	295.45	0.23	0.48	-0.25
2120	236.78	228.6	25.5	324.14	0.67	1.97	-1.30
8986	366.53	198.12	22.6	351.72	0.12	0.41	-0.29
3014	285.08	228.6	14.5	662.07	3.82	4.14	-0.32
4391	434.40	279.4	20	234.48	0.09	0.28	-0.19
11480	570.15	203.2	23.7	400.00	6.97	5.08	1.89
3896	377.39	254	23.1	317.24	4.48	4.06	0.42
4591	437.12	177.8	30.5	358.62	1.15	2.15	-1.00
7215	526.71	228.6	22.9	627.59	2.16	1.79	0.37

Table 3b. Inputs for Pavements on Stabilized Bases

Unconfined, kPa	KESAL	k, kPa/cm	PCC, mm	Shear, kPa	Fault, mm	Predicted, mm	Residual
11034.48	2137.00	532.14	198.12	482.76	0.29	0.31	-0.02
8034.48	8439.00	477.84	243.84	979.31	0.25	0.42	-0.17
12413.79	20584.00	904.095	198.12	558.62	0.21	0.46	-0.25
18655.17	19804.00	103.17	228.6	234.48	0.09	0.10	-0.01
17931.03	7451.00	268.785	243.84	344.83	0.11	0.36	-0.25
12413.79	10922.00	176.475	254	1165.52	1.42	1.41	0.01
13448.28	16082.00	447.975	254	482.76	0.8	0.49	0.31
14482.76	4114.00	453.405	304.8	503.45	0.06	0.31	-0.25
10482.76	5104.00	1001.835	203.2	1068.97	0.78	0.32	0.46
13275.86	8278.00	188.3124	243.84	193.10	0.27	0.26	0.01
13793.10	3060.00	942.105	203.2	1241.38	0.41	0.31	0.10
18517.24	2800.00	412.68	279.4	344.83	0.82	0.30	0.52
16896.55	2000.00	662.46	254	1579.31	0.03	0.31	-0.28
21931.03	2000.00	1009.98	228.6	696.55	0.15	0.30	-0.15
23068.97	977.00	754.77	228.6	641.38	0.26	0.30	-0.04

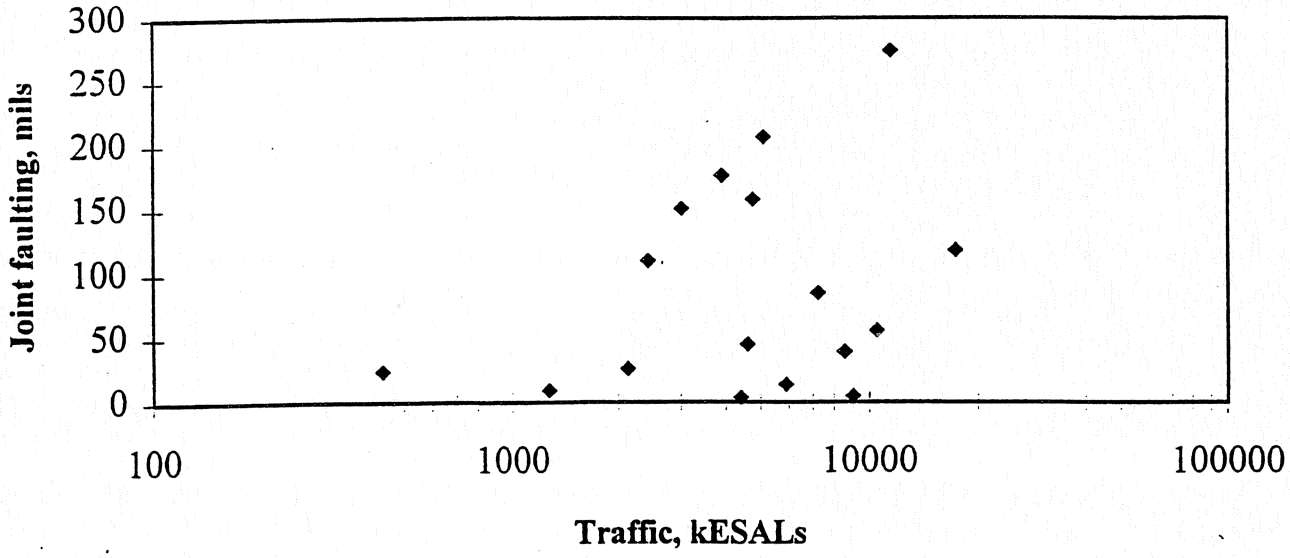


Figure 1. **Joint faulting versus traffic: crushed stone base (1mil=0.0254mm).**

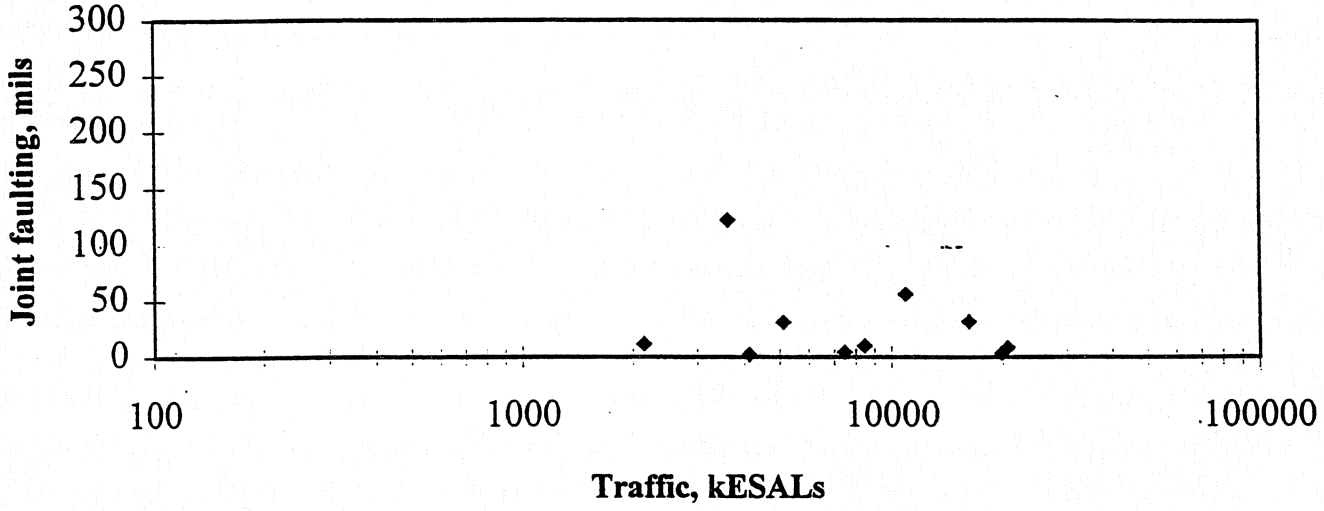


Figure 2. **Joint faulting versus traffic:cement-agg base (1mil=0.0254mm).**

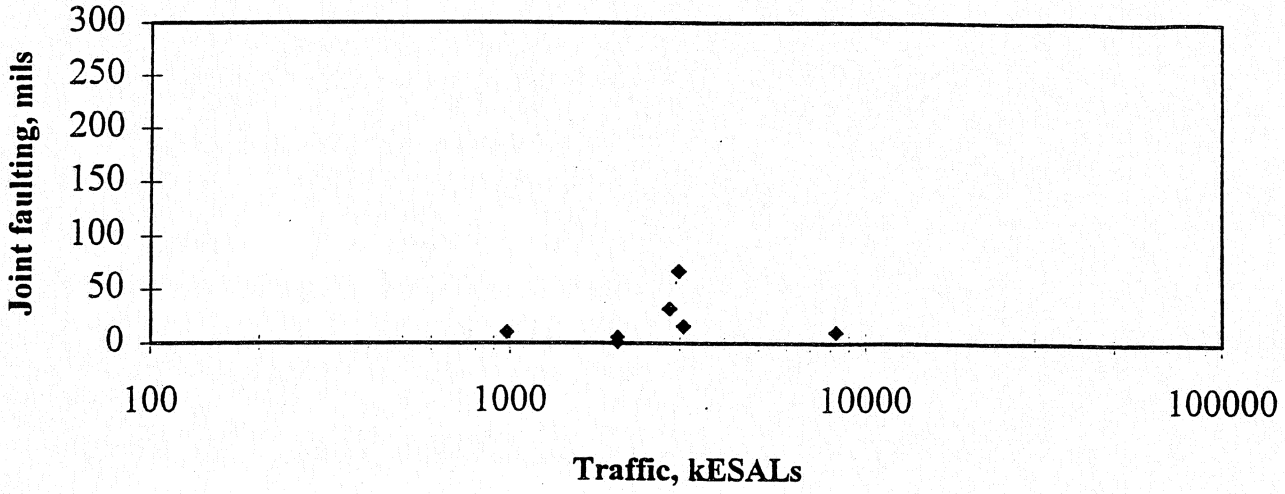


Figure 3. Joint faulting versus traffic:lean concrete base (1mil=0.0254mm).

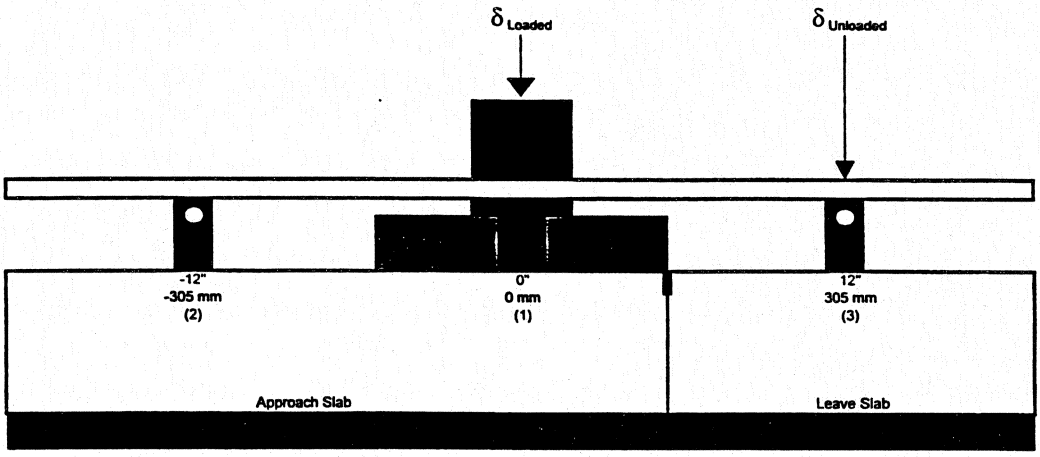


Figure 4. Definition of loaded and unloaded deflections.

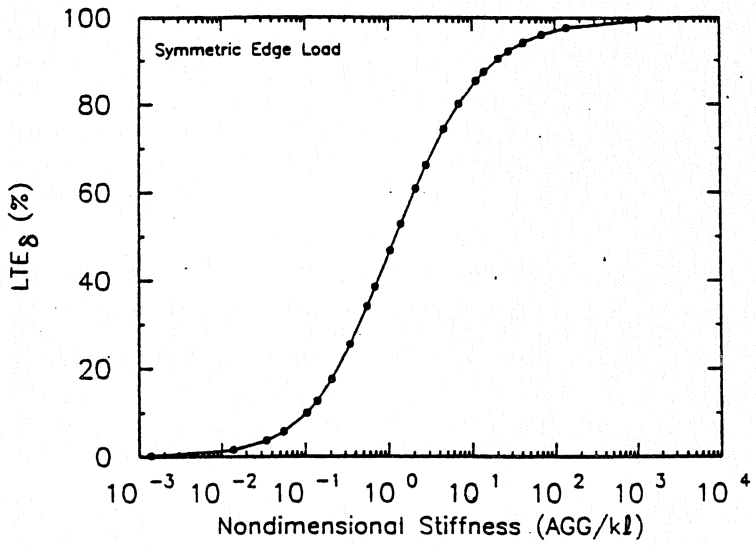


Figure 5. Relationship between LTE and AGG/kℓ (5).

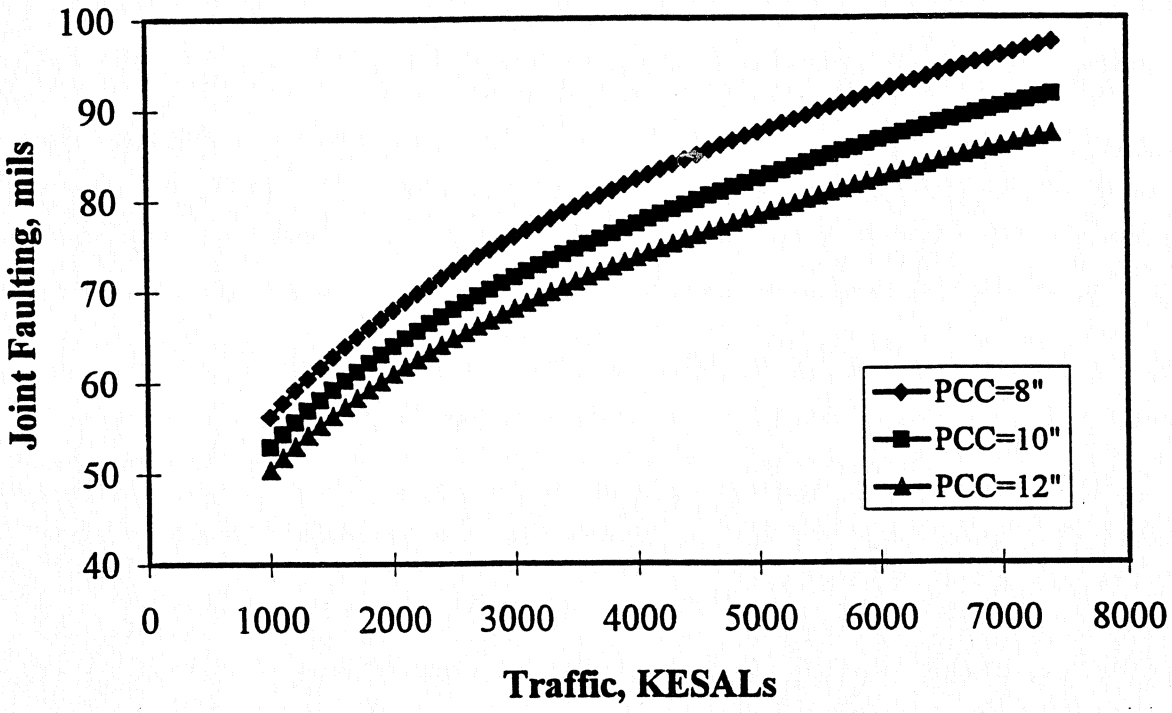


Figure 6. Sensitivity of joint faulting to traffic as a function of thickness (agg base) (1mil=0.0254mm; 1"=25.4 mm).

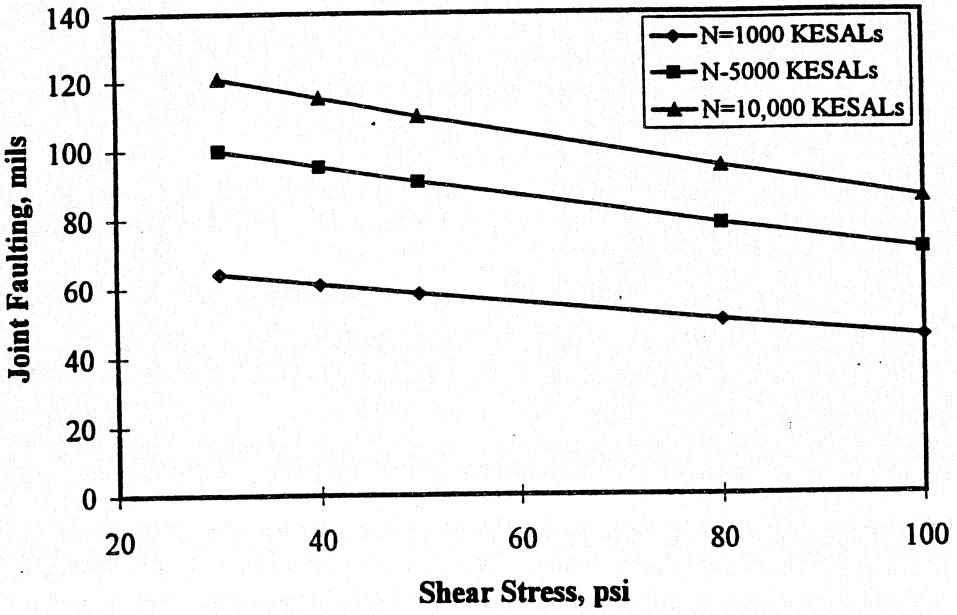


Figure 7. **Sensitivity of joint faulting to shear capacity as a function of traffic (agg base) (1mil=0.0254mm, 1"=25.4mm, 1 kPa = 0.145 psi).**

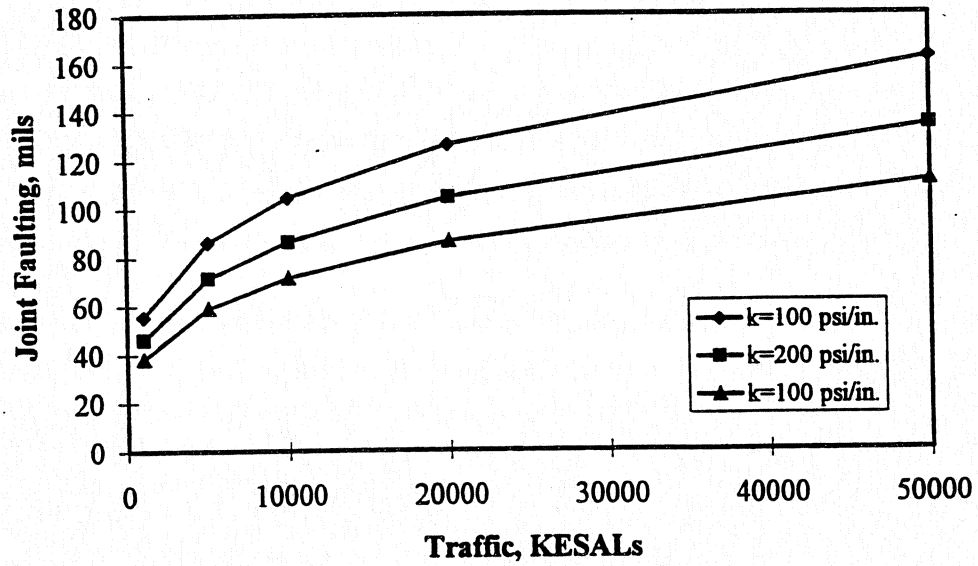


Figure 8. **Sensitivity of joint faulting to traffic as a function of subgrade support (agg base) (1mil=0.0254mm, 1"=25.4 mm, 100 psi/in=271.5 kPa/cm).**

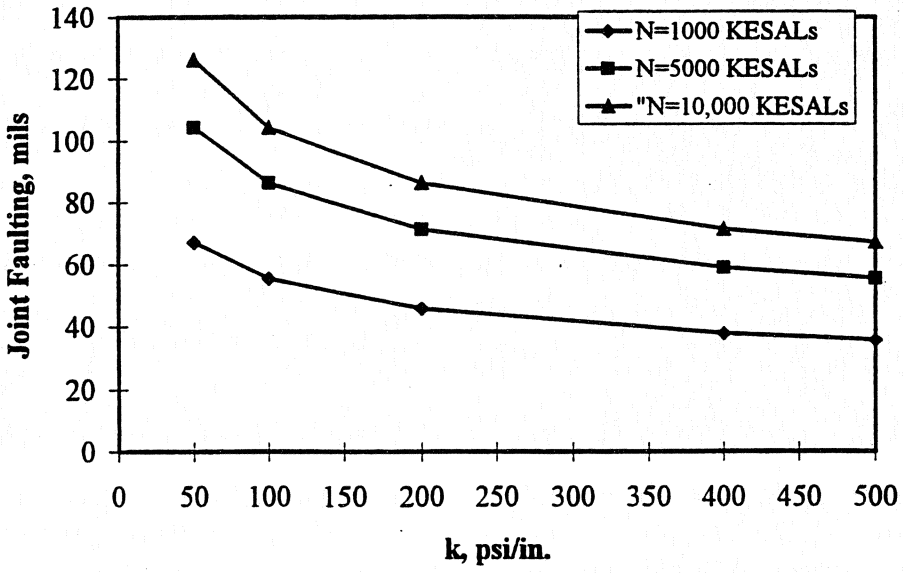


Figure 9. **Sensitivity of joint faulting to subgrade support (agg. base) (1mil=0.0254mm, 1"=25.4 mm, 100 psi/in=271.5 kPa/cm).**

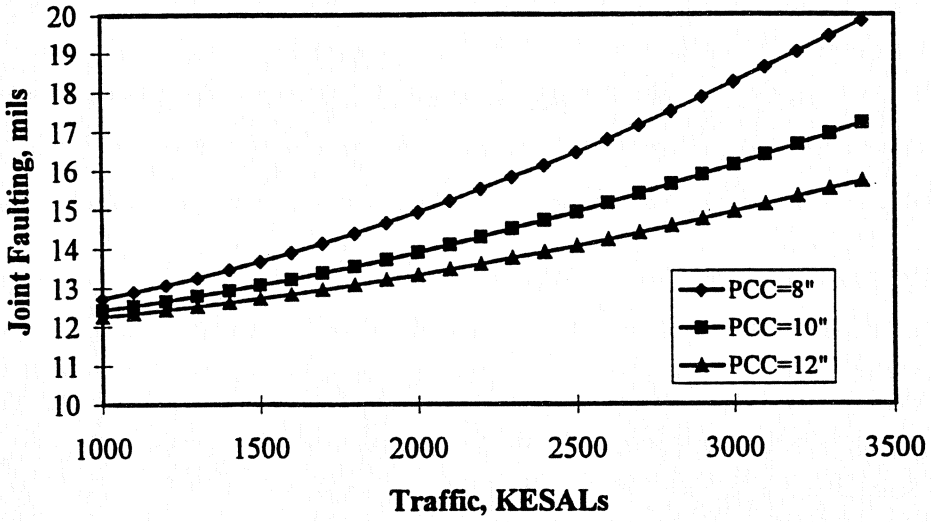


Figure 10. **Sensitivity of joint faulting to traffic as a function of pavement thickness (stabilized base) (1mil=0.0254mm, 1"=25.4 mm).**

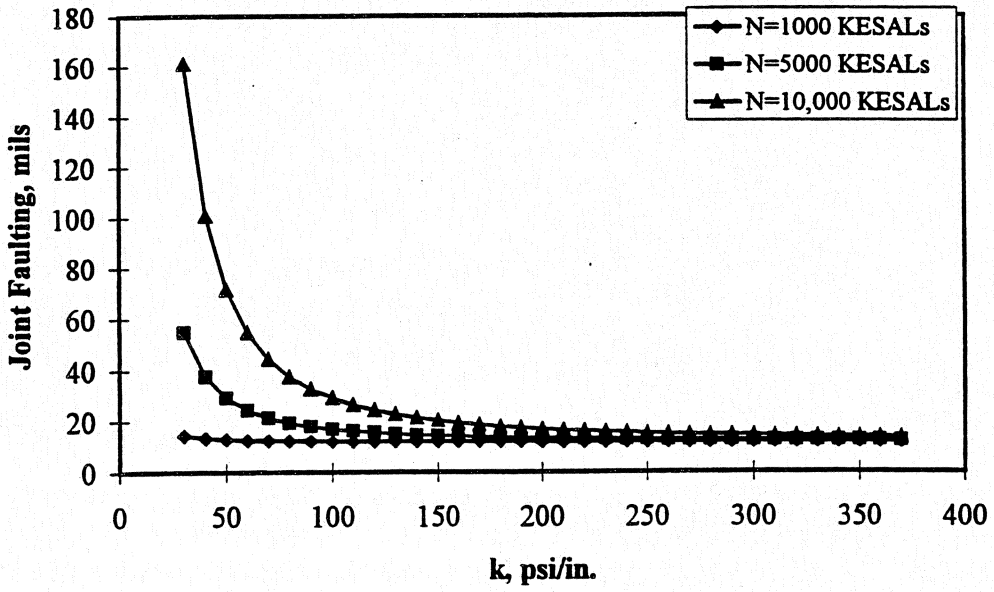


Figure 11. **Sensitivity of joint faulting to subgrade support as function of traffic (stabilized base) (1mil=0.0254mm, 1"=25.4 mm, 100 psi/in=271.5 kPa/cm).**

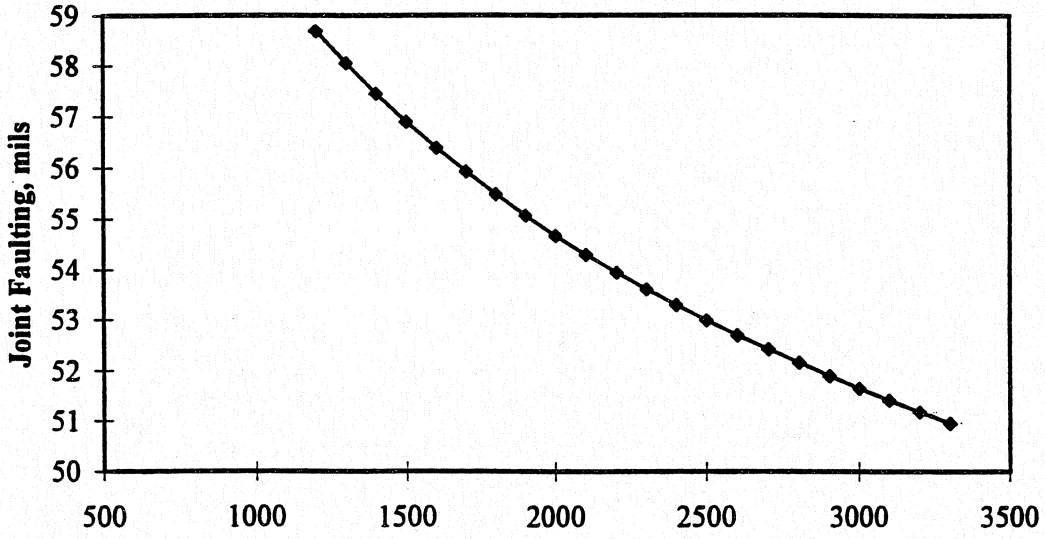


Figure 12. **Sensitivity of joint faulting to base strength (stabilized base) (1mil=0.0254mm, 1"=25.4 mm, 1kPa=0.145 psi).**

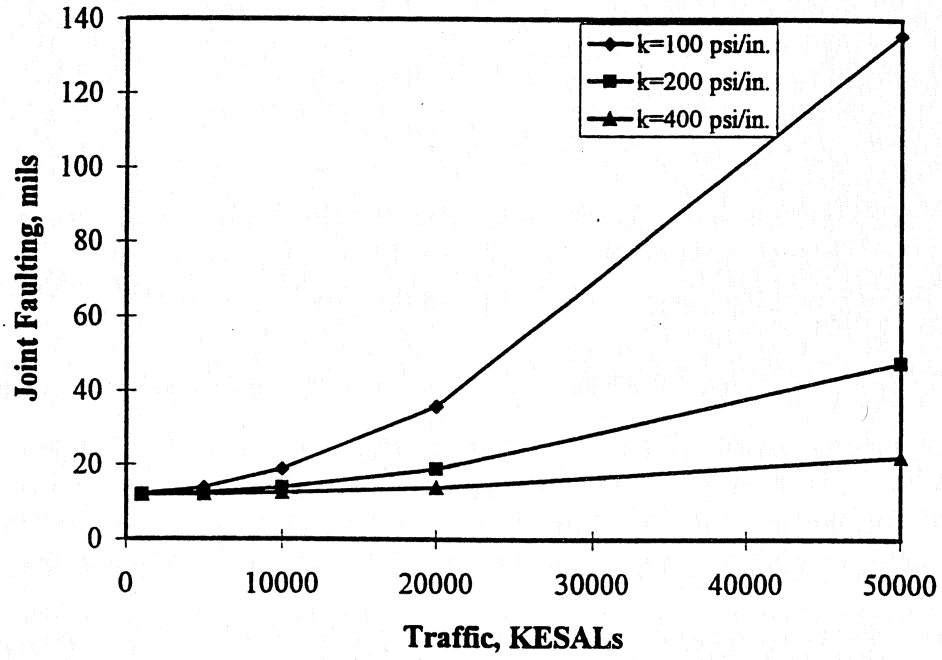


Figure 13. Sensitivity of joint faulting to traffic as function of subgrade support (stabilzed base) (1mil=0.0254mm, 1"=25.4 mm, 100 psi/in=271.5 kPa/cm).

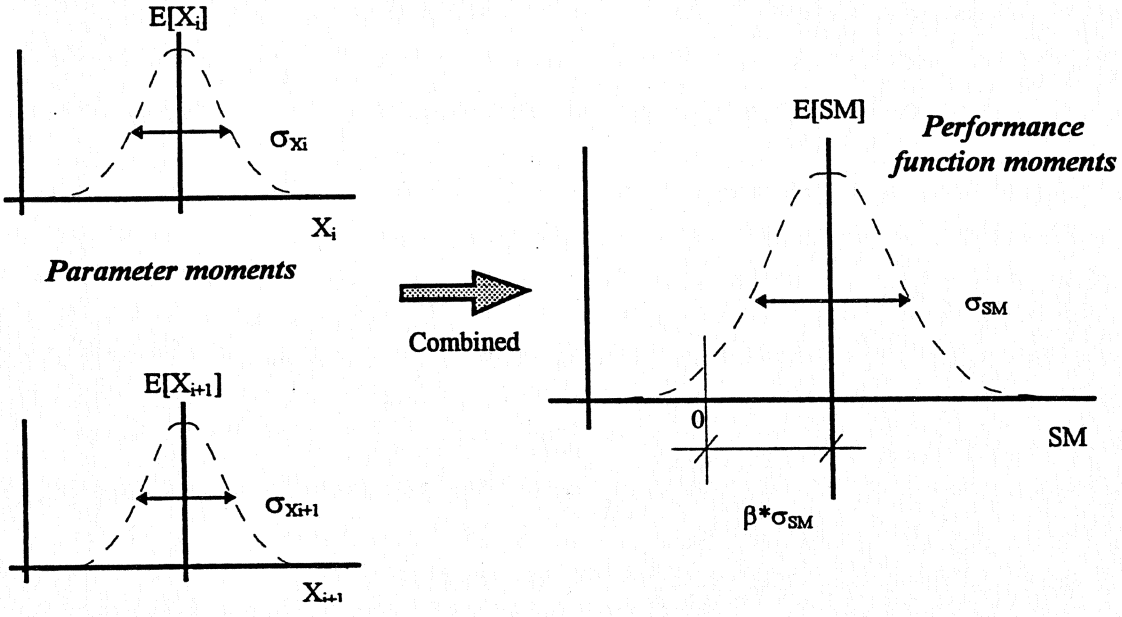


Figure 14. Fundamentals of Reliability Index.

REFERENCES

1. *SHRP-LTPP Overview: Five Year Report*, Strategic Highway Research Program, SHRP-P-416, National Research Council, Washington D.C., 1994.

2. *SHRP: Sensitivity Analysis for Selected Pavement Distresses*, Strategic Highway Research Program, SHRP-P-393, National Research Council, Washington D.C., 1994.

3. R.G. Packard, *Design Considerations for Control of Joint Faulting of Undoweled Pavement*, Proceedings of the First International Conference on Concrete Pavement Design, Purdue University, February 1977, pp. 121-136.

4. N.J. Buch, Development of Empirical-Mechanistic Based Faulting Models in the Design of Plain Jointed Concrete Pavements, *Ph.D. Dissertation*, Texas A&M University, College Station, August 1995.

5. A.M. Ioannides, Y.H. Lee, & M.I. Darter, *Control of Faulting Through Joint Load Transfer Design*, TRR 1286, Transportation Research Board, Washington D.C., 1990, pp.49-57.

6. M.I. Darter, K.T. Hall, and C. Kuo., *Support Under Portland Cement Concrete Pavements*, NCHRP Report 372, Transportation Research Board, Washington, D.C., 1995.

7. *SPSS® for Windows™ Base System*, Release 6.0, SPSS Inc., Chicago, Illinois.

8. G.N. Smith, *Probability and Statistics in Civil Engineering: An Introduction*, Nichols Publishing Company, New York, 1986.